nature geoscience

SUPPLEMENTARY INFORMATION

DOI: 10.1038/NGEO1047

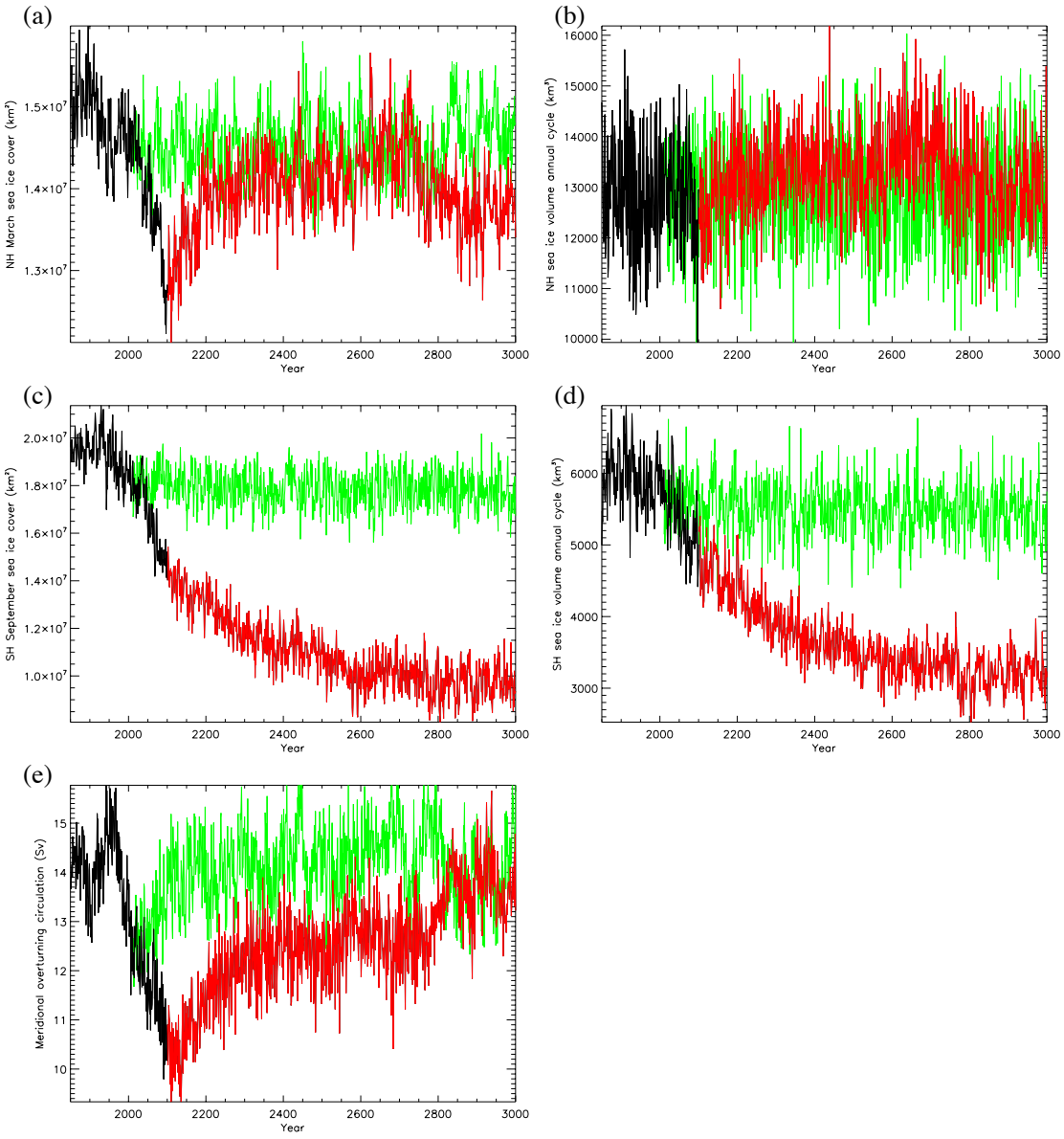

Figure S1 Timeseries of the sea ice and overturning circulation response to a cessation of CO_2 emissions. Northern Hemisphere March sea ice cover (km^2) (**a**), Northern Hemisphere annual cycle in sea ice volume (km^3) (**b**), Southern Hemisphere September sea ice cover (km^2) (**c**), Southern Hemisphere annual cycle in sea ice volume (km^3) (**d**), and Atlantic meridional overturning circulation strength (Sv) (**e**), in the HIST/SRES (black), ZE2010 (green), and ZE2100 (red) simulations. Sea ice cover is shown in the months of maximum ice extent in each hemisphere.

DOI: 10.1038/NGEO1047

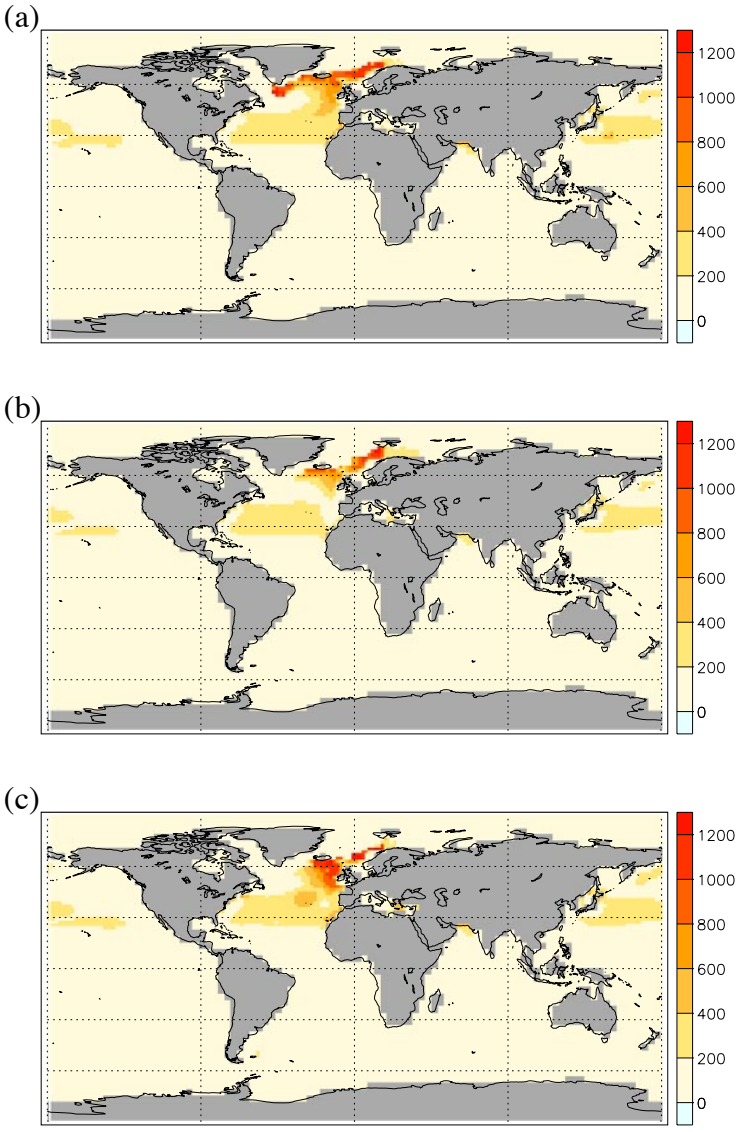

Figure S2 March mixed layer depth in 1855, 2105 and 2995 in m. Decadal mean March mixed layer depths are shown in HIST/SRES in 1855 (**a**), in ZE2100 in 2105 (**b**), and in ZE2100 in 2995 (**c**). Mixed layer depths in 1855 closely resemble the observed climatology[1]. Deep mixed layers (> 1000 m) are indicative of regions of deep water formation. The mean surface temperature in March in such deep water formation regions is 6.1°C in 1855, 7.9°C in 2105 and 10.9°C in 2995.

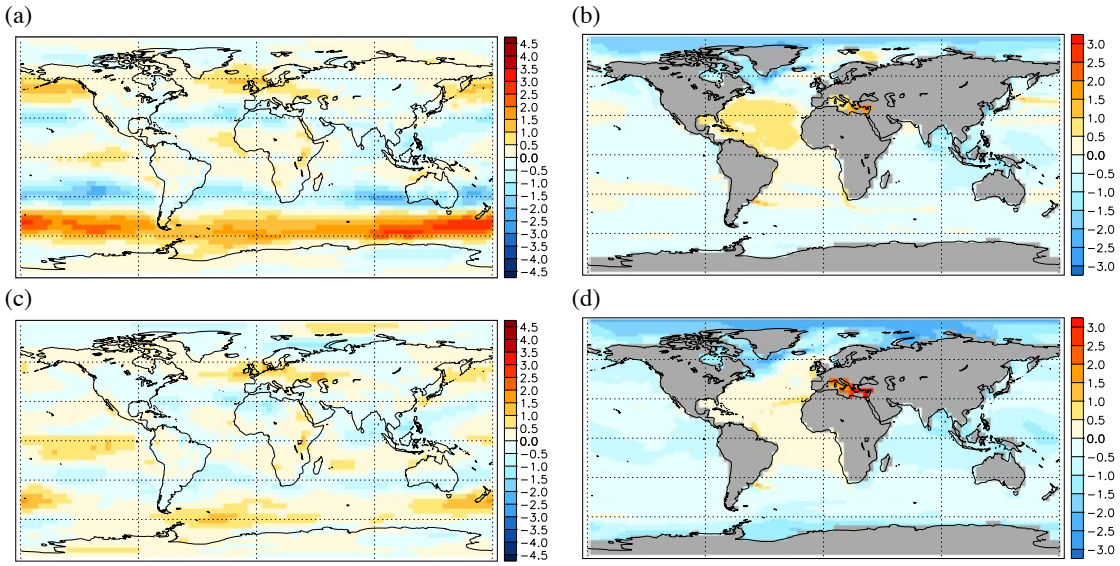

Figure S3 Simulated anomalies in 1000-hPa zonal wind and sea surface salinity in 2105 and 2995. 1000-hPa zonal wind change between 1855 and 2105 (ms^{-1}) (**a**), sea surface salinity change between 1855 and 2105 (PSU) (**b**), 1000-hPa zonal wind change between 1855 and 2995 (ms^{-1}) (**c**), and sea surface salinity change between 1855 and 2995 (PSU) (**d**) in HIST/SRES and ZE2100. All changes are calculated as a difference of decadal means centred on the specified years.

DOI: 10.1038/NGEO1047

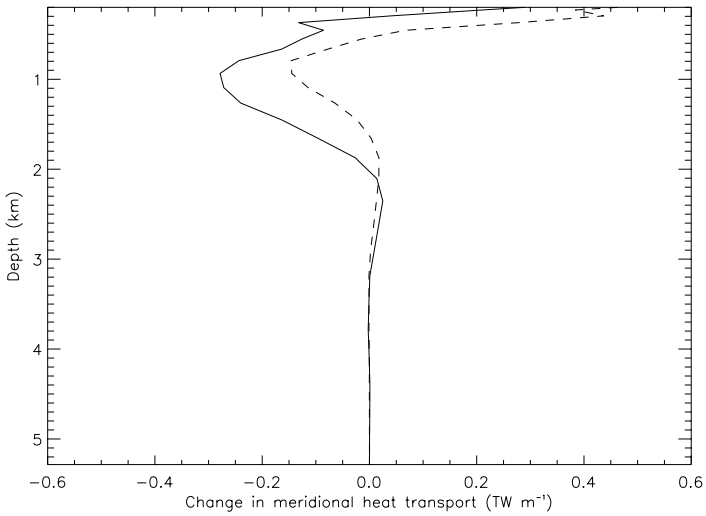

Figure S4 Meridional ocean heat transport change on the equator as a function of depth. Zonal mean northward equatorial meridional heat transport change between 1855 and 2105 (dashed) and between 1855 and 2995 (solid) in HIST/SRES and ZE2100 (TW m^{-1}). Only the heat transport change corresponding to the steady component of the ocean flow below 200 m depth is shown.

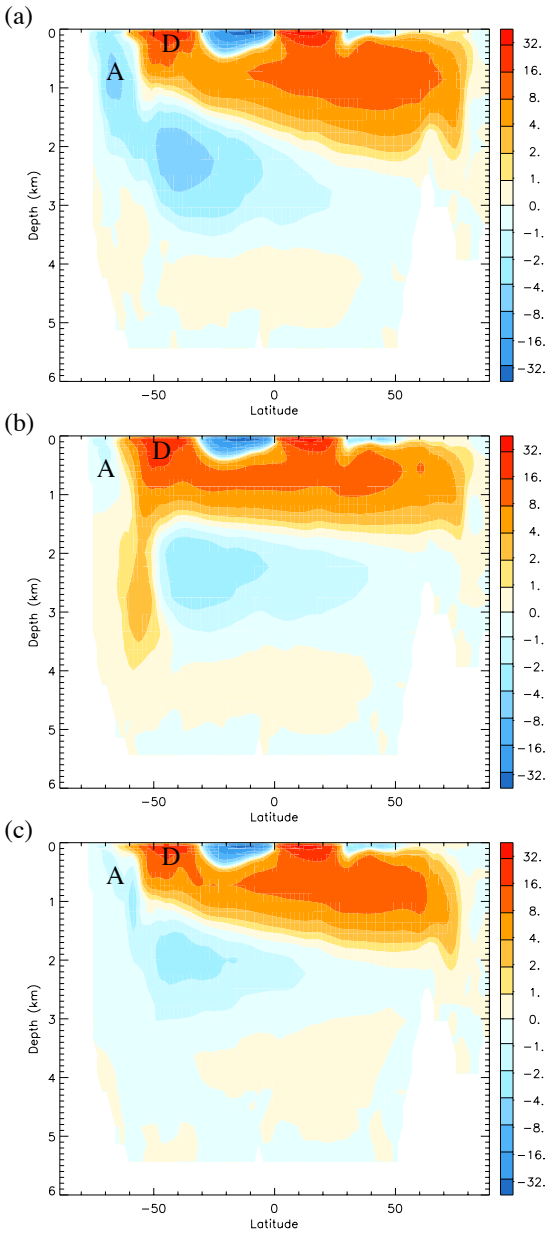

Figure S5 Tracer meridional overturning streamfunction in 1855, 2105 and 2995. Meridional overturning streamfunction (Sv), accounting for transport by the simulated meridional velocity and the bolus velocity, which represents transport by parameterised eddies, in 1855 (**a**), 2105 (**b**), and 2995 (**c**) in HIST/SRES and ZE2100. A and D indicate the locations of the Antarctic Bottom Water Overturning Cell, and the Deacon Cell respectively. Stream functions are decadal means centred on the specified years. Note that the colour scale is logarithmic.

DOI: 10.1038/NGEO1047

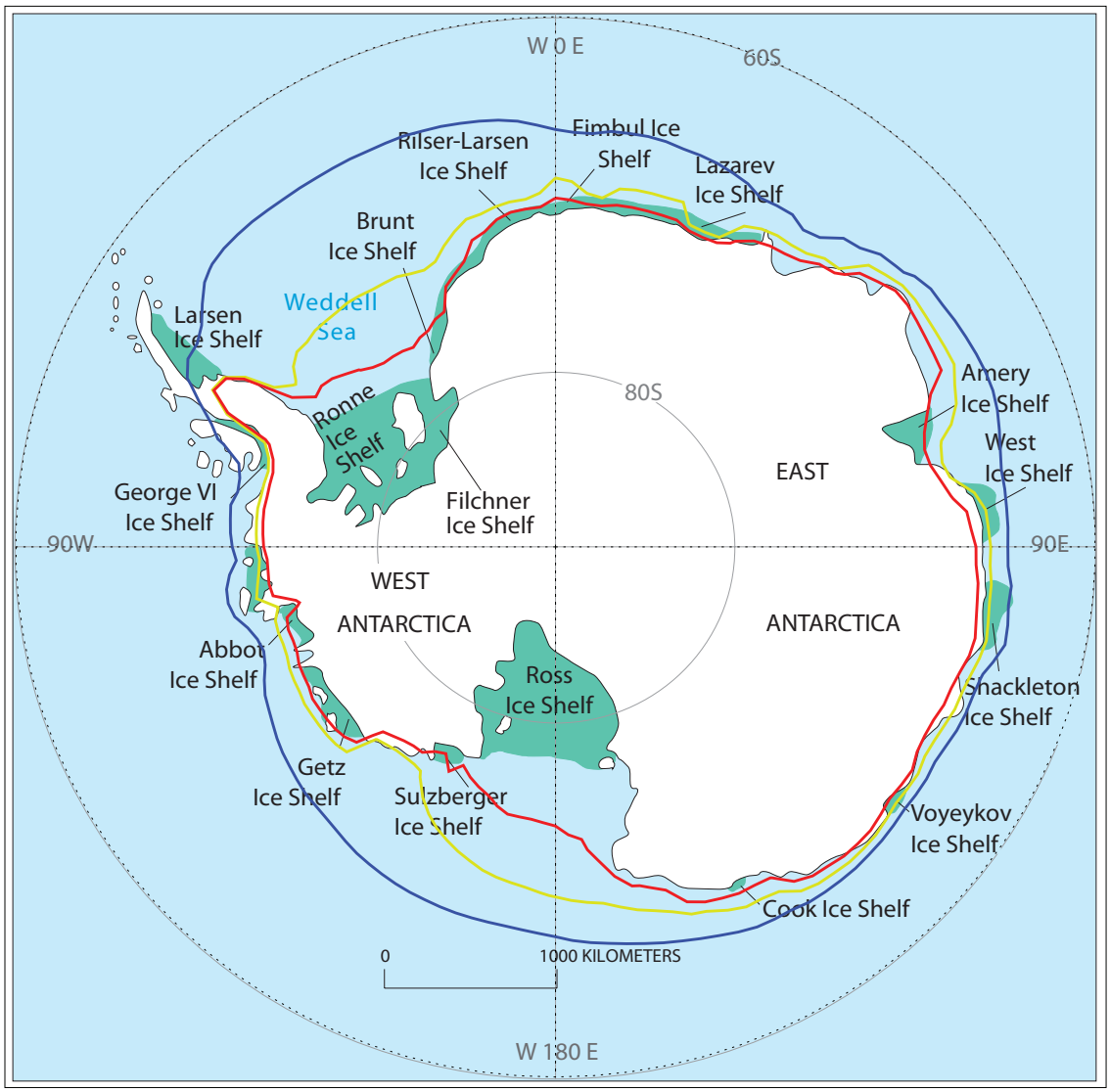

Figure S6 Annual mean -9°C isotherm in 1855, 2105 and 2995. The -9°C near-surface temperature isotherm is shown in 1855 in HIST/SRES (blue), in 2105 in ZE2100 (light green) and in 2995 in ZE2100 (red), where simulated temperatures have been bias-corrected relative to the ERA40 1979-2001 climatology. The surface air temperature-controlled geographic limit for ice shelves is well-approximated by the -9°C annual mean isotherm[2]. Isotherms are superposed on a map of Antarctic ice shelves[3].

Supplementary References

1 Levitus, S., *Climatological atlas of the world ocean*. (National Oceanic and Atmospheric Administration, Princeton, N.J., 1982).

2 Morris, E. M. & Vaughan, D. G. in *Antarctic Peninsula climate variability: historical and paleoenvironmental perspectives* (eds Domack, E. W. *et al.*) (American Geophysical Union, 2003).

3 Williams, R. S. J., Ferrigno, J. G. & Foley, K. M. *Coastal-Change and Glaciological Maps of Antarctica*, <http://pubs.usgs.gov/fs/2005/3055/> (2009).